International Journal of Psychosocial Rehabilitation, Vol. 24, Issue 05, 2020
ISSN: 1475-7192

Diagnosis of Brain Tumor using Semantic Segmentation and Advance-CNN Classification

A. Afreen Habiba and B. Raghu

Abstract--- *The brain cancer prediction is mediocre at an early stage as it is impotent by the radiologist. Various investigations done so far manifest clearly that the nodule segmentation algorithms are ineffectual. Thus, this investigation has centralized semantic segmentation based Nano segmentation method for precise segmentation of lesion. The supreme intent of this research paper is the enhancement of brain MRI images to recognize the tumor efficiently and small-scale anomalous nodules segmentation in the brain region. The initial step Isolateral filter enhancement techniques which can eradicate the noise discern in the images. In the subsequent step the semantic Segmentation Based Nano area detection algorithm is implemented in an enhanced nodule image sequence for abnormal brain tissue prediction. Ultimately, the brain nodule images are procured by utilizing a deep learning based Advanced CNN (ACNN). Nano Segmentation method and the deep learning classification (DLC) method has an accuracy of 95.7% that helps to diagnose the cancer cells using the feature extraction process which is done automatically. Average segmentation time for nodule slice order is 1.01s. Comparative analysis is made with ResNet-50 based on the different testing and training data at the rate of 90% -10%, 80%-20% and 70%-30% respectively which proves the robustness of the proposed research work. Experimental results prove the proposed system effectiveness when compared with other detection methods.*

Keywords--- *Isolateral Filter, Semantic Segmentation Based Nano algorithm, Advanced CNN.*

I. INTRODUCTION

Unanticipated demises are predominantly engendered due to cancer. Various international scrutinized logbook manifests that brain cancer tops the chart in the prompt for death in Homo sapiens. It can be de-escalated by prior diagnosis so that pertinent treatment can be prescribed by the oncologists in a stipulated period. Obstreperous burgeon found in a group of cells causes cancer and the malignant tumor is formed by invading the tissues. In this paper, Brain cancer, MRI scan images are preferred. AMRI scan or Computerized Axial Tomography (CAT) scan is the most sensitive and peculiar recognition modality affords cross-sectional images for precise areas of scanned objects [12]. The target of this research is to configure a system in which MRI images are fed as inputs and desired outputs are attained. The proposed algorithm is well-organized with reference to sensitivity, specificity, and accuracy [6]. In literature point of view, several researchers proposed various methods for automated detection of pulmonary nodules.

Nevertheless, all the existing methods must undergo four processes in order to the detection of pulmonary nodule which include preprocessing, segmentation, feature extraction, and classification. Magnetic Resonance Image (MRI)

A. Afreen Habiba, Habiba Research Scholar, Department of Computer Science and Engineering, Bharath University, Chennai (Tamil Nadu), India.
B. Raghu, Principal and Professor, Department of Computer Science and Engineering, SVS Group of Institutions, Warangal (Andhra Pradesh), India. E-mail: habiba.afreen@gmail.com

DOI: 10.37200/IJPR/V24I5/PR201795
Received: 13 Feb 2020 | Revised: 07 Mar 2020 | Accepted: 23 Mar 2020

provides an expedient diagnoses of the pulmonary nodules when compared to X-ray. The DNA existing in certain cells are not renovated after impairment rather these cells grow and form new abnormal cells, such cells are known to be cancerous cells, [1], [4], & [12]. Brain cancer is an antagonistic and heterogeneous disease and is the prime cause of cancer-related demises comparatively. The occurrence of abnormal cells leads to brain cancer [3], & [5] that cluster together to form a tumor (nodule).

Every tumor will not be categorized under cancerous [9], & [13]. The non- cancerous tumors are known as benign nodules. The other cancerous nodules that grow without particular sequence, resistor and obliterate the healthy brain tissues around them are called malignant nodules [6], & [8].

Two categorizations of brain cancer are [10], & [18] (i) Small Cell Brain Cancer (SCLC) which is composed of 10% to 15% of all brain cancers and (ii) Non-Small Cell Brain Cancer (NSCLC) which shares 80% to 90% of brain cancers. A Computer Aided Detection System (CAD) [12], [14], & [9] are one among the predominant investigation streams in medical imaging and diagnostic radiology. A dominant Computer Aided Diagnosis aids in processing image for recognition and eradicating the anomalies and also assist the classification of image features between normal and anomalous [15], & [19]. A CAD system is instrumental in reducing the number of erroneous diagnosis [3], & [22]. The feat of a CAD system is measured in terms of accuracy, sensitivity & specificity in diagnosis, speed and its degree of automation. Computer-aided diagnosis [23] & [25] based on artificial neural network is implemented in the classification of the brain cancer [1], [6], & [19].

The key attributes considered during classification includes area, perimeter, and shape. The extreme classification attained is about 90%. For the classification few methods based on the content based Image Retrieval (CBIR) [11], [17], & [21] have been stated. New framework [2] is proposed for open source pulmonary nodule image retrieval purpose. Here the system extracts the images of the individual nodules from the LIDC collection and calculates the Haralick co-occurrence [23], Gabor filters and Markov random field features [16], & [27] of the nodules. Retrieval make use of distance measure which comprise of a Euclidean, Manhattan, and Chebychev. The extreme retrieval rate procured is to be 88%.

Pontribution of the Proposed Research include:

i. The proposed **Iso-lateral** technique automatically provides segmentation of an block into sub regions with definite textures or color patches without knowing the number of regions in advance whereas the existing pre-processing technique concentrates on noise as in [20]*(Rajeev, Sanjay Sharma, and S. K. Sharma).*

ii. Advantage of using **Semantic segmentation** in the proposed research is that it effectively determines the set of seed points, thereby avoiding the chances of overlap. The proposed clustering methods provides the grouping of similar pixel values together with similar intensity values while the existing methodology deals with the localized seed point model as in [21]. *(Abdel-Maksoud, Eman, Mohammed Elmogy).*

iii. Proposed **Nano** Segmentation is proposed that overcomes the limitations existing in [30] by proper clustering and the segmentation of the brain for the extraction of cancer cells.

DOI: 10.37200/IJPR/V24I5/PR201795
Received: 13 Feb 2020 | Revised: 07 Mar 2020 | Accepted: 23 Mar 2020

iv. In-order to demonstrate the effectiveness of the proposed technique, the SS based segmentation is carried out for higher accuracy with better segmentation results when compared to the other segmentation methods [15],[28],[34].

v. One of the most proven **Deep learning technique using Resnet-50** is used for classification to classify the tumor as benign or malignant, that yields better accuracy by reducing the false positives, whereas most of the existing techniques provide a high false positive rate as in [22] that in turn assist the radiologists to diagnose the cancer at an early stage more accurately.

vi. An in-depth comparative analysis with various performance measures in case of both segmentation and classification is carried out to demonstrate the effectiveness of the proposed system.

The organization of the paper is given by the following sections: At Section II The image acquisition method is described where the image is acquired from the scanners at the biomedical centers. The preprocessing stage is done where the resizing along with color conversion occurs followed by the **Iso-lateral filter** and Segmentation involving the new method of proposed **semantic segmentation** and the proposed **Nano segmentation** method. The final Step of Classification is done with Feature Extraction and **deep learning** Methodology. Section III provides performance measures, section IV explains the result analysis and section V gives an evaluation of performance values.

II. PROPOSED METHOD

In the first instance the target of the propounded method is to enhance and segment the pulmonary nodule. Eventually the segmented nodules are categorized by dual cutting-edge methods, chronicle approach of these methods are provided explicated in the upcoming sections.

A. Proposed Algorithm for Iso-Lateral Filter

The set schema underneath displays the proposed technique deals with brain image. At the outset the image acquisition is performed by capturing images required or attain those images from the **open source database**. In this research open source dataset, **Brain Image Database Consortium (BIDC)** is preferred. The Publicly available BIDC MRI scans of 50 patients, which include 650 nodules tested and **in-house clinical dataset** of 80 patients with 505 MRI images.

The initial step of the proposed novel technique is to preprocess the brain image hinge on the **Isolateral filtering (IF)**method. While preprocessing, an input MRI image undergoes noise eradication engendered during image generation which in turn eliminates the undesirable signals which can entail certain errors in the course of processing.

The brain MRI scan images are mostly nobbled by certain noise which integrates Gaussian noise, visual noise and speckle noise. In conjunction with contrast enhancement the noise eradication must be performed on the MRI image to execute an improved medical image diagnosis. The **Isolateral filtering** (IF) is preferred to eliminate the Gaussian noise.

DOI: 10.37200/IJPR/V24I5/PR201795
Received: 13 Feb 2020 | Revised: 07 Mar 2020 | Accepted: 23 Mar 2020

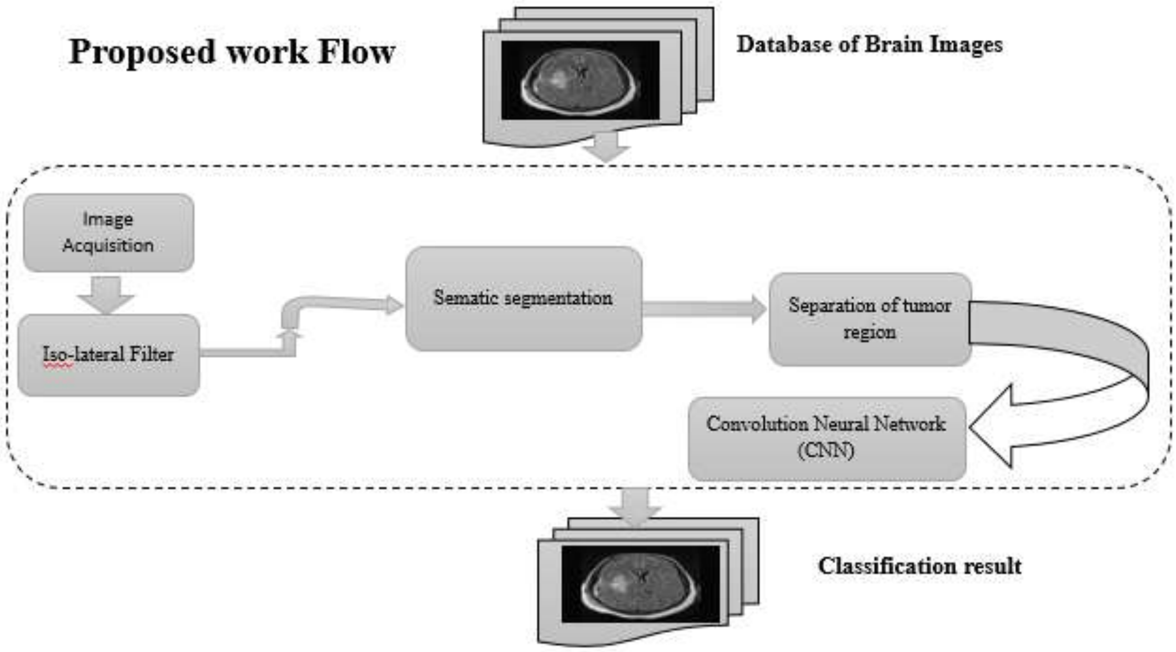

Fig. 1: Block Diagram for Proposed Method of Brain Nodule Image Segmentation

The quality of the images is labelled as poor due to certain deficiencies spotted in the image, thus the speckle & visual noise can disturb the quality of those images. The presence of speckle noise is unpleasant since it spoils the quality of the image, and affects the tasks of individual interpretation and diagnosis. Speckle noise is a multiplicative noise, therefore it's hard to eliminate this noise compared to additive noise. The traditional techniques are incompetent in reducing certain noises, particularly speckle noise. Hence a supplementary filter is being annexed to target on speckle noise reduction. **Isolateral filtering (IF) with the unsharp masking technique** is put into practice in this research for eliminating the annoying noise detected in the input MRI brain images and for image enhancement technique. Over here the image is craigslist into three subparts: Black, Gray and White. Consequently the quality of images can be enhanced and thereby stipulates an ideal detection of the tumor region existing in the images. Ultimately, the preprocessed images are attained effectually.

Algorithm: Isolateral Filter

Step 1: Convert input image to double.
Step 2: Initially calculate the Gaussian distribution function.
Step 3: Initialize the weight of the Gaussian distribution.
Step 4: Calculate Euclidean distance of each pixel value.

The new pixel level value (k) is calculated for each of the brightness values in the original image, as given in Equation (1),

$$k = \sum_{i=0}^{j} N_i / T \quad (1)$$

Where the sum calculates the number of pixels by determining the integration of the histogram with brightness less than term *j* and T is the total pixel value.
Step 5: Calculate the finite difference after which distribution function is evaluated.

DOI: 10.37200/IJPR/V24I5/PR201795
Received: 13 Feb 2020 | Revised: 07 Mar 2020 | Accepted: 23 Mar 2020

B. Proposed Algorithm for Semantic Segmentation based Nano Segmentation (SS)

The supreme target of super pixel based algorithm is to cluster pixels with a homogenous appearance of an image into a compact region. The super pixel segmentation may provoke a clustering quandary because each super pixel comprises of unique features in color and shape.

A novel algorithm, termed as semantic segmentation (SS) that clusters pixels in the amalgamated form of three-dimensional colors such as, black, white and gray is being propounded in this investigation.

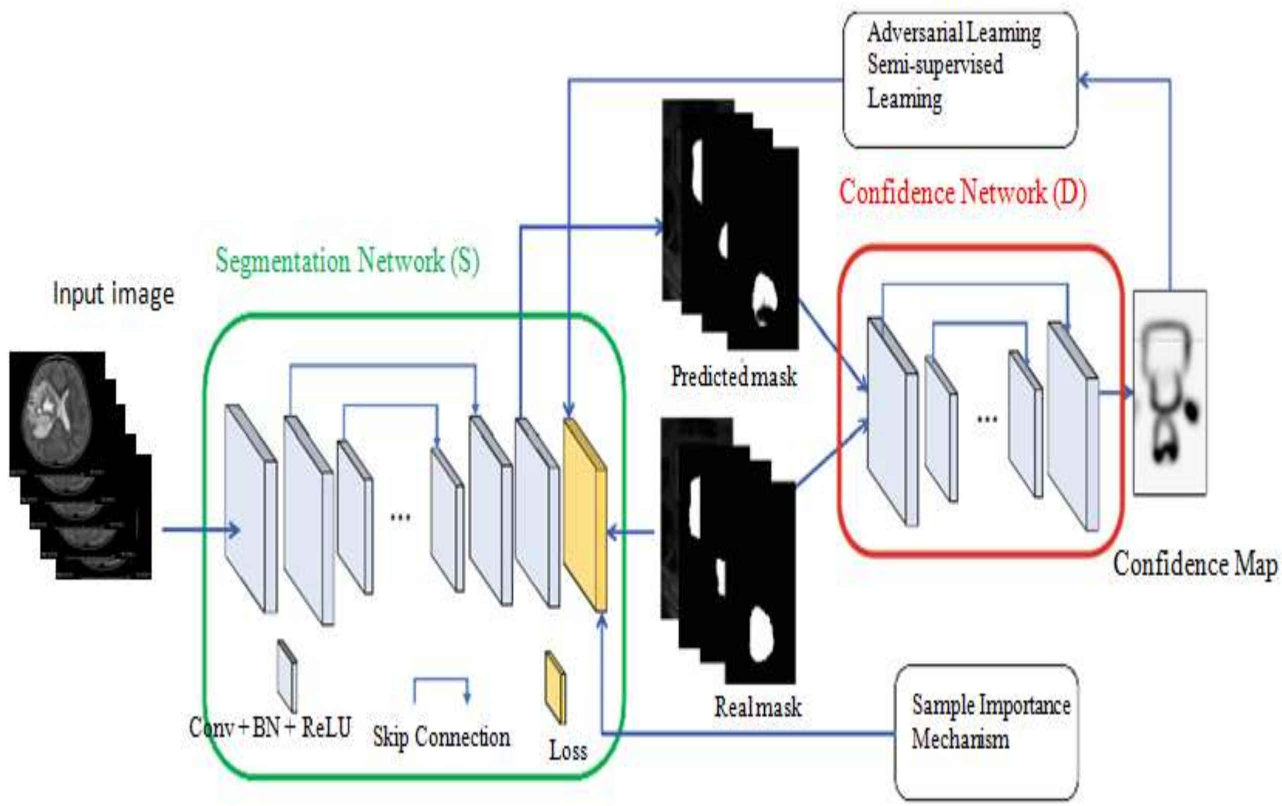

Fig. 2: Proposed Flow Diagram for Semantic Segmentation

Dual stages are involved in the proposed method - a clustering stage and a merging stage. In the inceptive stage the pixels are being aggregated to procure initial super pixels. The subsequent stage involves in refining these initial super pixels and attain the final super pixel by merging very small super pixels with the help of the iterative clustering method.

The effortlessness of the favored methodology gives a remarkably simple approach for unique utilization, where the parameter specifies the number of super pixels and the efficiency of the algorithm is relatively high. Experiments result makes it clear that the preferred approach yields better segmentation output when compared to the existing supper pixel approach [47, 48, 49&50]. Algorithm 1, describes about the proposed semantic segmentation (SS) method.

DOI: 10.37200/IJPR/V24I5/PR201795
Received: 13 Feb 2020 | Revised: 07 Mar 2020 | Accepted: 23 Mar 2020

Algorithm 1: Semantic Segmentation (SS)

Step 1: Input Image Initialization Process

Initialize cluster center $C_k = [L_k, a_k, b_k, x_k, y_k]^T$ in the hexagonal grid, pixels label matrix l, distance matrix D from pixels to cluster centers, hexagonal grid spacing S and radius r of circular structure element

Step 2: Move Cluster center

initial cluster center to the smallest gradient position in the hexagonal region.

Step 3: Repeat Process

Repeat the same condition

While residual error > = threshold E do

If the residual error greater than or equal to threshold Do the for condition

For each cluster center C_k do

Obtain sub image cluster center & Distance calculation process

Obtain sub images (use $[x_k, y_k]$ as the center, 2*S as the side) containing cluster centers. Calculate the distance between each pixel in the sub image and cluster center. If the distance is less than the previous value, then update its l and D

End for End the for condition

Update the cluster center

Calculate the mean of [equation 1] L, a, b, x and y of each super pixel to update the cluster center. Recalculate the residual error, go to the third step, and continue the execution

End while End the While condition

Step 4: Mask Prediction Process

Obtain all non-connected regions of the MRI image and then perform the open operation of the circular structure element radius r. The final result is subtracted from the original MRI image denoted as mask

Step 5: Perform distance transform

Perform distance transform on mask, and assign each small region to the nearest super pixel

Step 6: Computation Process

Compute the super pixel adjacency matrix for subsequent operation. Until all CT image sequences are segmented

Step 7: Obtained Output.

Execute connection operations and sequential output

$$d_{lab} = \sqrt{(l_k - l_i)^2 + (a_k - a_i)^2 + (b_k - b_i)^2} \quad (2)$$

$$d_{xy} = \sqrt{(x_k - x_i)^2 + (y_k - y_i)^2} \quad (3)$$

$$D_s = d_{lab} + (m / S)*d_{xy} \quad (4)$$

Where, Distance measure D_s is shown in the equation (4).

D_s is the sum of the lab distance and the xy plane distance normalized by the grid interval S. A variable m is introduced in D_s which can control the compactness of super pixel. The greater the value of m, the more spatial proximity is emphasized and the cluster becomes more compact. This value can be in the range [1, 20]. Authors of the algorithm have chosen m=10.

DOI: 10.37200/IJPR/V24I5/PR201795
Received: 13 Feb 2020 | Revised: 07 Mar 2020 | Accepted: 23 Mar 2020

C. *Proposed Classification algorithm based on neural network (Advance resnet 50- Convolution Neural Network)*

ResNet 50 is preferred to pre train CNN and can extract features in the input image fed to the network. The principal focus of using the ResNet 50 is to train millions of images. The core benefits of ResNet 50 is that it encompasses residual connections, which evades the information loss during the training process. Thus the speed of processing can be enhanced by using ResNet in CNN training.

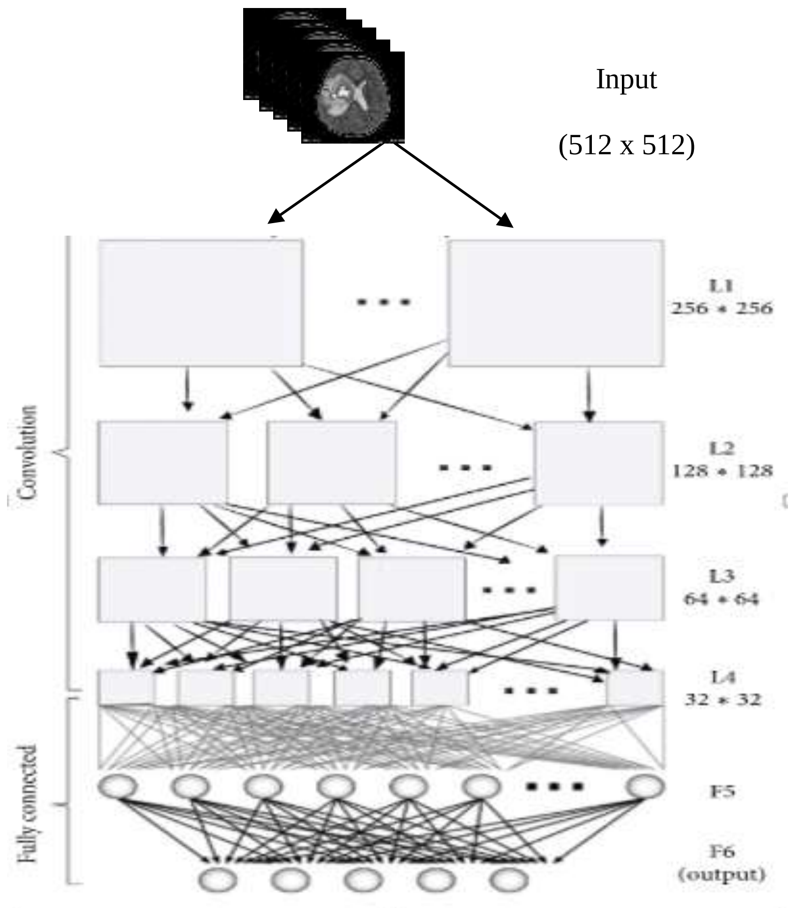

Fig. 3: Flow diagram of Convolution Neural Network

CNN used for classification comprises of three convolutional layers, three pooling layers, and two fully connected layers (***Fig.3***). When experimentations are accomplished, the CNN is being trained by means of the original database. The image initially enters into the first convolution layer. The top left of the image determines the input matrix initiation.

Subsequently the software picks a minor matrix which is renowned as filter. Convolution is being implemented by dint of this filter, i.e. collaboratively moves with the input image. The filter's value multiplies with the original pixel values. The products acquired are summed up together to attain the ultimate value. Only the upper left corner

DOI: 10.37200/IJPR/V24I5/PR201795
Received: 13 Feb 2020 | Revised: 07 Mar 2020 | Accepted: 23 Mar 2020

of the image is read by the filter hence, it moves further towards the right by 1 unit and then the comparable operation is being executed.

Once the filter crosses all the position, a matrix is formed nevertheless the obtained matrix is smaller compared to the input matrix. The output of the classifier can be either benign or malignant type. Algorithm 3 expounds the proposed Advanced Convolutional Neural Network Algorithm (resnet 50-CNN).

Algorithm 3: Advanced Convolutional Neural Network Algorithm (ACNN)

Begin

Set condition of i=1

Iteration 1 and then generate R ← random number (between 1 to NumGW).Calculate the first three best fit values

Check condition R

Check condition R from a database (both public and in-house clinical) of numbers so that R should not repeat. Update the value.One by one data points are taken from TestData .Set as an position

Position ← Test Data(R)

Pass Position to CNN as input,assigns a point *x* to the class of its closest neighbour in the feature space and get CNN Output. (Fitness evaluation

Calculate Parameters

such as, Accuracy ← Target Value – CNN Output

Best_Value ← Accuracy

Best_Position ← Position

Then do, i=2 Iteration 2for each grey wolf NumGW. Replace worst fit gray wolf value with best fit

Check condition if (Best_Value> Accuracy)

Then Calculate alternatively, Best_Value=Accuracy

Best_Position=Position

Get the best solution with best fitness gray wolf value.

End for

End

III. PERFORMANCE MEASURES

The performance of the proposed algorithm has been evaluated in terms of Peak signal-to-noise ratio (PSNR), Mean Square Error (MSE) and Structural Similarity Index Method (SSIM).

Equation (5) estimates the **mean-squared error** to compute PSNR

$$MSE = \sum_{M_1,N_1} \frac{[I_1(m_1,n_1) - I_1(m_2,n_2)]^2}{M_1 \times N_1} \quad (5)$$

M1 and N1 are the number of rows and columns in the input images, respectively. The equation (6) computes PSNR,

$$PSNR = 10 log_{10}\left(\frac{R1^2}{MSE}\right) \quad (6)$$

International Journal of Psychosocial Rehabilitation, Vol. 24, Issue 05, 2020
ISSN: 1475-7192

The **SSIM index** is calculated on various windows of a brain image. The measure between two window x and y common size N×N. Equation (6) shows the computation of the SSIM index.

$$SSIM(x,y) = \frac{(2\mu1_x\mu1_y+c_2)(2\sigma1_{xy}+c1_2)}{(\mu1^2._x+\mu1^2._y+c_1)(\sigma1x^{1\,2}+\sigma1y_2+C1_2)} \quad (7)$$

Where,$\mu1_x$ the average of x_i

$\mu1_y$the average of y_i

$\sigma1x^2$the average of x_i

$\sigma1y^2$the average of y_i

$\sigma1_{x,y}$the covariance of x and y.

$$C_1 = (K_1L)^2), C_2 = (K_2L)^2)$$

Dice: The relationship involving ground truth 'G' and segmented image 'F' such that, it computes the ratio of the common to the sum of the number of elements between them.

$$. Dice = \frac{2|G \cap F|}{|G| + |F|} \quad (8)$$

IV. Results and Discussion

The results acquired by implementing SSBIC are being estimated in this section. Images are obtained from BIDC or from in-house clinical database. Initially, image processing is performed on the image which are being estimated and are aided by the simulation results which are being accomplished using **MATLAB 2019a**. **Fig.4** and **Fig.5** displays the sample images. Here 10 brain cancer MRI scan image are attained from public BIDC database.

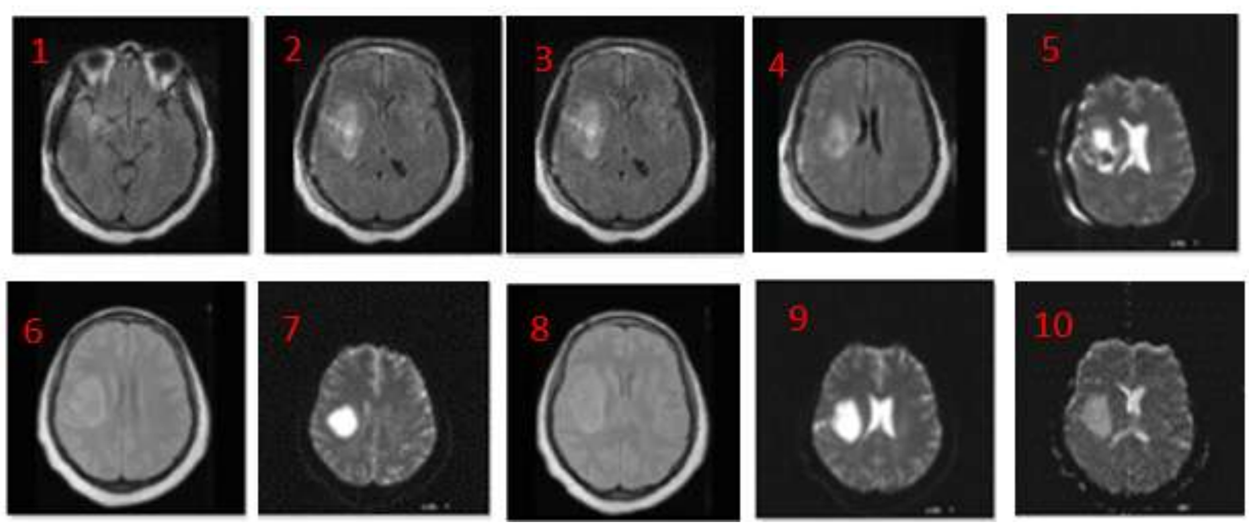

Fig. 4: Sample 10 Public LIDC Database Image

DOI: 10.37200/IJPR/V24I5/PR201795
Received: 13 Feb 2020 | Revised: 07 Mar 2020 | Accepted: 23 Mar 2020

International Journal of Psychosocial Rehabilitation, Vol. 24, Issue 05, 2020
ISSN: 1475-7192

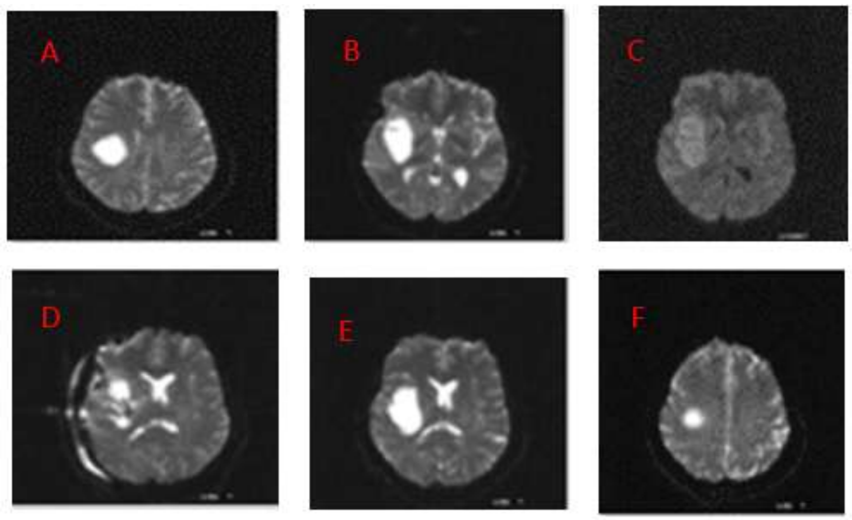

Fig. 5: Sample 6 In-house Clinical Database Image (Pranav Diagnosis Centre in Nagercoil)

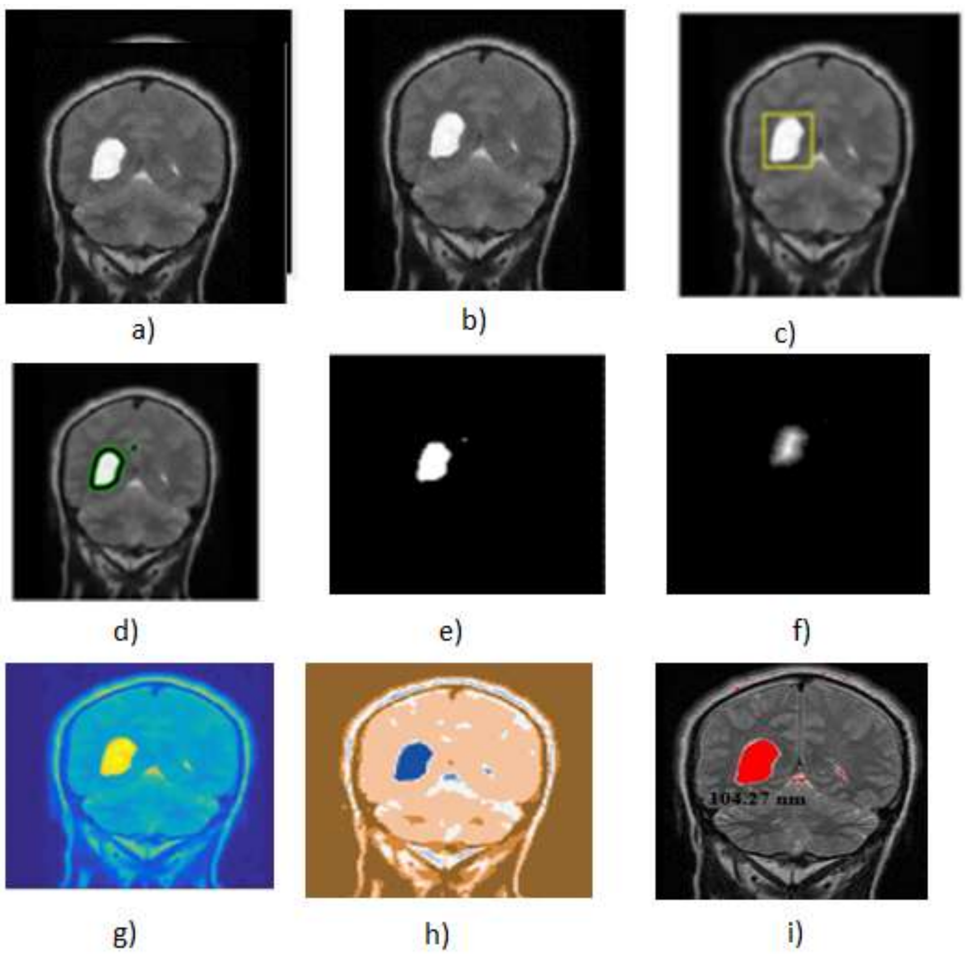

Fig. 6: Experimental Result of Benign Brain Tumor Image (a)Brain Image of Tumor Affected Brain (b)Isolaeral Filter Image (c) Locating Seed Box Image (d) Semantic Segmentation Image (e) Segmented Tumor Region Image (f) SSBIC Image (g) Semantic Segmentation Coloring Image (h)Nano Image

DOI: 10.37200/IJPR/V24I5/PR201795
Received: 13 Feb 2020 | Revised: 07 Mar 2020 | Accepted: 23 Mar 2020

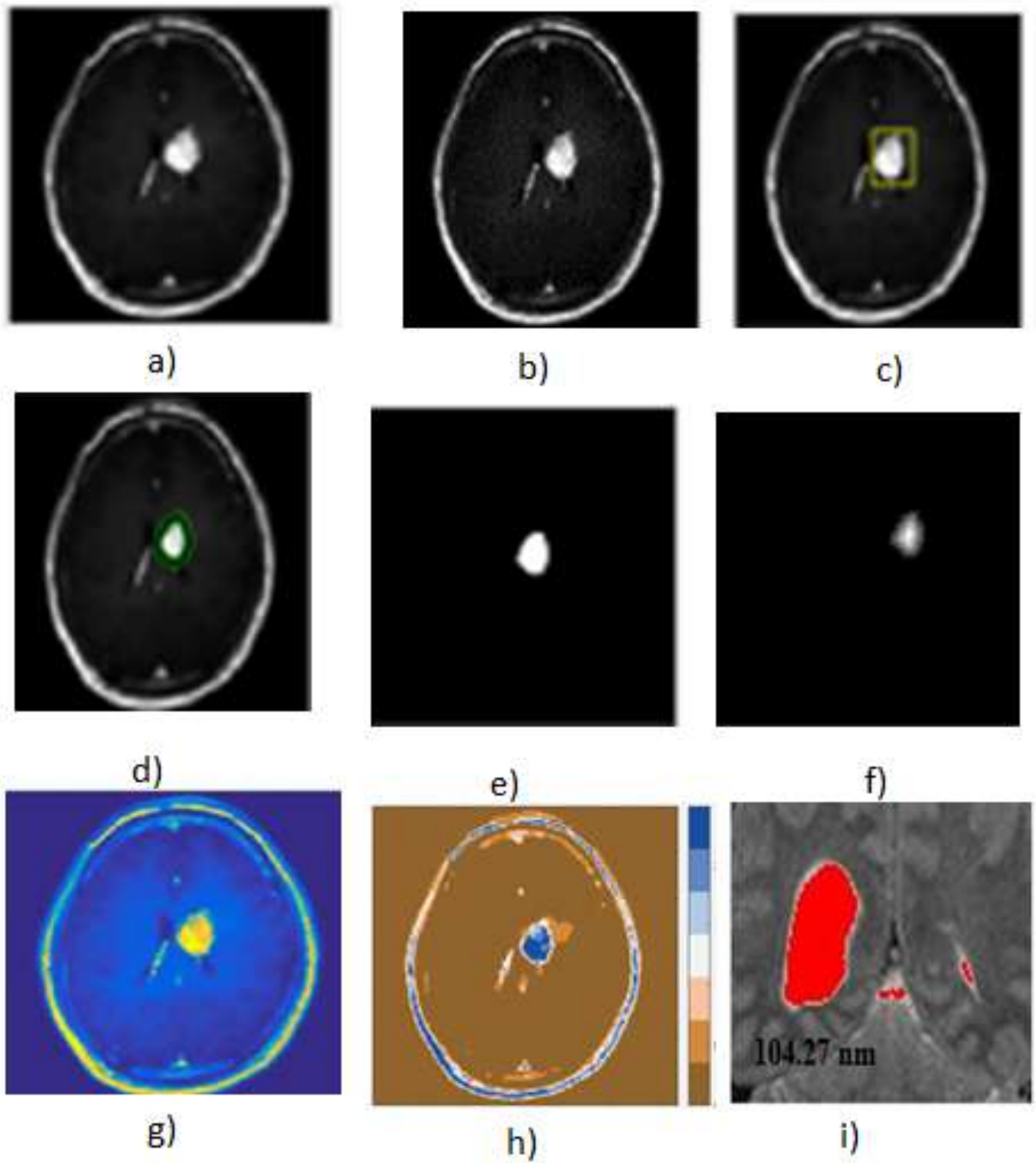

Fig. 7: Experimental Result of Malignant Brain Tumor Image (a)Brain Image of Tumor Affected Brain (b) Isolaeral Filter Image (c) Locating Seed Box Image (d) Semantic Segmentation Image (e) Segmented Tumor Region Image (f) SSBIC Image (g) Semantic Segmentation Coloring Image (h) Nano Image

Table 1: Performance Analysis of Pre-processing

Metrics	**Anisotropic Filter**	**Bilateral Filter**	**Proposed method**
PSNR	26.56	30.68	35.92
SSIM	0.7823	0.8453	0.9125
MSE	0.0044	0.0028	0.00052

DOI: 10.37200/IJPR/V24I5/PR201795
Received: 13 Feb 2020 | Revised: 07 Mar 2020 | Accepted: 23 Mar 2020

Table 2: Summarizes the Effect of Varying Threshold and 'i' Values on the Accuracy of Solitary Nodules Detected. 'N' is the Number of Solitary Nodules Detected

Dataset	**Threshold**	**i=10**		**i=10**	
		A-CNN		**-CNN**	
		Accuracy	**N**	**Accuracy**	**N**
Publically available BIDC Dataset	0.65	97.0	44	97.6	44
	0.75	85	38	85	38
	0.85	66.67	20	66.7	20
In-house Clinical Dataset	0.65	90.7	34	92.5	34
	0.75	82	27	85.33	30
	0.85	60.76	21	62.15	24

On varying the threshold value there is an effect on the number of solitary nodules detected in widely available BIDC Dataset and In-house Clinical Dataset (Table 2). The threshold value is proportional to accuracy.

Table 3: Segmentation Performance Measures of Dice Parameter

Images	**Dice**			
	Otsu segmentation	**Fuzzy C Means clustering**	**Watershed Segmentation**	**Proposed SS Method**
Sample 1	0.0036	0.1472	0.0045	**0.1520**
Sample 2	0.0052	0.2295	0.0030	**0.2459**
Sample 3	0.0026	0.2086	0.0052	**0.1965**
Sample 4	0.0036	0.2426	0.0123	**0.2993**
Sample 5	0.0014	0.1611	0.0053	**0.1526**
Sample 6	0.0060	0.1639	0.0040	**0.2337**
Sample 7	0.0047	0.144	0.0045	**0.174**
Sample 8	0.0011	0.2114	0.0012	**0.165**
Sample 9	0.0015	0.1774	0.0034	**0.147**
Sample 10	0.0014	0.166	0.0012	**0.159**
Sample 11	0.0016	0.244	0.0032	**0.1357**
Sample 12	0.0011	0.144	0.0014	**0.1258**
Sample 13	0.0015	0.2354	0.0074	**0.147**
Sample14	0.0030	0.177	0.0094	**0.1357**
Sample 15	0.0064	0.166	0.0041	**0.2147**
Sample 16	0.0041	0.1254	0.0045	**0.2413**
Sample 17	0.0056	0.1337	0.0054	**0.247**
Sample 18	0.0021	0.1247	0.0041	**0.195**
Sample 19	0.0023	0.100	0.00624	**0.1854**
Sample 20	0.0041	0.2654	0.0081	**0.17354**
Average	0.0037	0.1922	0.0057	**0.2133**

DOI: 10.37200/IJPR/V24I5/PR201795
Received: 13 Feb 2020 | Revised: 07 Mar 2020 | Accepted: 23 Mar 2020

Table 4: Segmentation Performance measures of SSIM Parameter

Images	SSIM			
	Otsu segmentation	**Fuzzy C Means Clustering**	**Watershed Segmentation**	**Proposed SS method**
Sample 1	0.0001	0.9653	0.9087	**0.9681**
Sample 2	0.0001	0.9842	0.9154	**0.9853**
Sample 3	0.0001	0.9730	0.9405	**0.9767**
Sample 4	0.0001	0.9641	0.9353	**0.9774**
Sample 5	0.0001	0.9422	0.9083	**0.9423**
Sample 6	0.0001	0.9391	0.9448	**0.9726**
Sample 7	0.0001	0.9613	0.9255	**0.9704**
Sample 8	0.0001	0.9612	0.904	**0.97554**
Sample 9	0.0001	0.9648	0.9541	**0.97665**
Sample 10	0.0001	0.9601	0.9621	**0.98110**
Sample 11	0.0001	0.9675	0.9004	**0.98115**
Sample 12	0.0001	0.9628	0.9341	**0.97221**
Sample 13	0.0001	0.9637	0.98100	**0.954**
Sample14	0.0001	0.9677	0.9554	**0.97164**
Sample 15	0.0001	0.9644	0.9113	**0.9784**
Sample 16	0.0001	0.9651	0.9733	**0.97314**
Sample 17	0.0001	0.9643	0.9510	**0.9745**
Sample 18	0.0001	0.9650	0.93241	**0.9527**
Sample 19	0.0001	0.9688	0.9277	**0.9688**
Sample 20	0.0001	0.9651	0.9557	**0.9714**
Average	0.0001	0.9613	0.9255	**0.9704**

Fig. 8 shows that the confusion matrix output from the ACNN classifiers. In this figure, the first two diagonal cells illustrate the number and percentage of precise classifications by the trained network. For example, 444 brain cancer images are unerringly classified as benign [31-38]. This corresponds to 63.5 % of all 699 brain cancer images. Similarly, 234 cases are unerringly classified as malignant.

This parallels to 33.5 % of all brain cancer images. 7 of the malignant brain cancer images are erringly classified as benign and this corresponds to 1.0 % of all 699 brain cancer images in the data. Consistently, 14 of the benign brain cancer images are erringly classified as malignant and this corresponds to 2.0% of all data. Out of 451 benign prognoses, 98.4% are unerring and 1.6% is erring [39-45].

Out of 248 malignant prognoses, 94.4 % are unerring and 5.6% are erring. Out of 458 benign cases, 96.9% are unerringly prognosis as benign and 3.1% are prognosis as malignant. Out of 241 malignant cases, 97.1 % are unerringly classified as malignant and 2.9 % are classified as benign. Overall, 97.0 % of the predictions are precise and 3.0% are erroneous.

DOI: 10.37200/IJPR/V24I5/PR201795
Received: 13 Feb 2020 | Revised: 07 Mar 2020 | Accepted: 23 Mar 2020

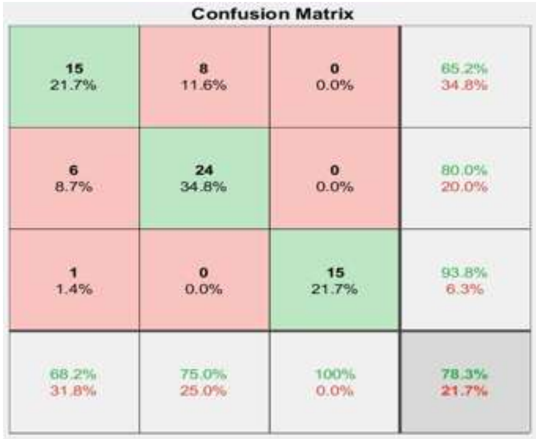

Confusion matrix for 60: 40

Confusion matrix for 70: 30

Confusion matrix for 85: 15

Confusion matrix for 90: 10

Fig. 8: The Confusion Matrix Output from the Advance CNN Classifiers

700 brain cancer images are nominated to execute classification process. A confusion matrix of 3x3 presents the output of **ACNN** classifier which estimates the accuracy of the image. The confusion matrix output from the **ACNN** classifiers **(Fig.9)**. The benign category includes 444 brain cancer images which are classified precisely. This corresponds to 63.5 % of all 699 brain cancer images. On the contrary, the malignant category includes 238 cases that are classified accurately. Thus 34.0 % of all brain cancer images has been categorized efficaciously. Nevertheless 3 brain cancer images must come under malignant brain cancer category, but they are erroneously classified as benign and this corresponds to 0.4 % of all 699 brain cancer images in the data [46-53]. In the exact same fashion, 14 brain cancer images ought to be classified under benign brain cancer images, but they are erroneously classified as malignant and equates to 2.0% of all data. If 447 benign undergo prognosis, 99.3% are unerring and 0.7% is erring. When 252 malignant prognoses are involved, 94.4 % are unerring and 5.6% are erring. Out of 458 benign cases, 96.9 % is unerringly determined as benign and 3.1% are prophesied as malignant. Out of 241 malignant cases, 98.8 % are accurately classified as malignant and 1.2 % is classified as benign. Overall, 97.6 % of the predictions are precise and 2.4% are erroneous.

DOI: 10.37200/IJPR/V24I5/PR201795
Received: 13 Feb 2020 | Revised: 07 Mar 2020 | Accepted: 23 Mar 2020

Confusion matrix 80: 20

Fig. 9: The Confusion Matrix Output from the A-CNN Classifiers

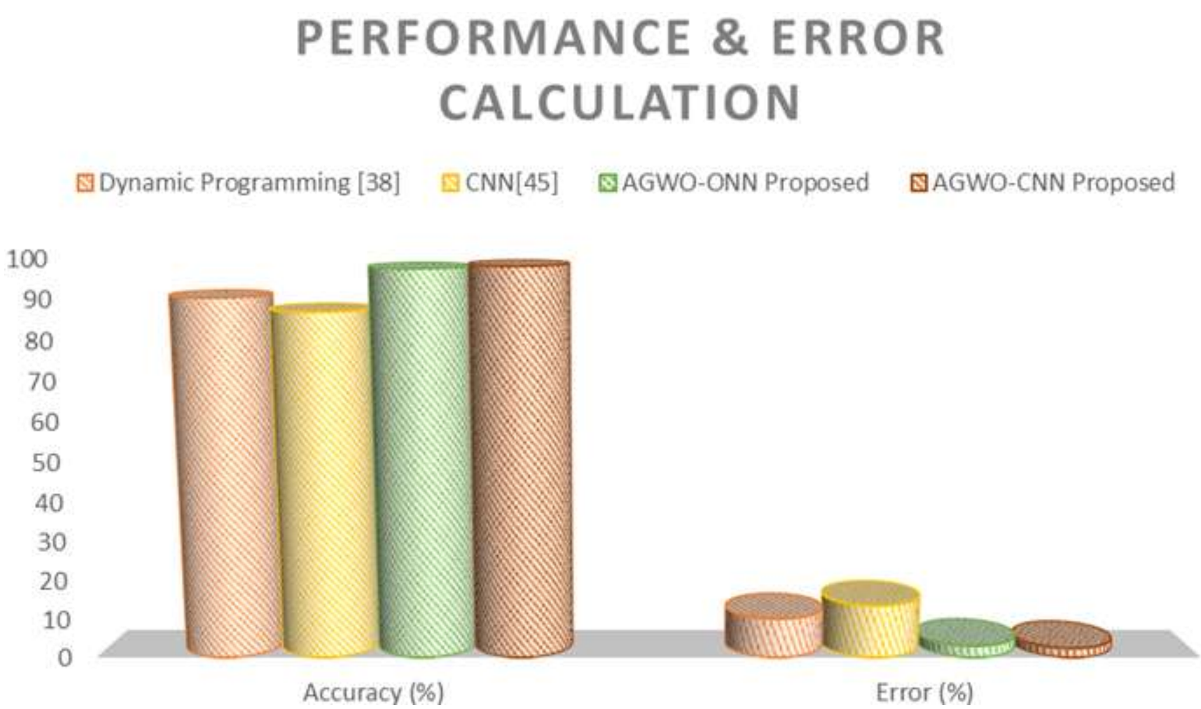

Fig. 10: Performance Comparison of the Proposed Technique and Existing Technique

In Fig.10 demonstrates that the accuracy is elevated for A-CNN classifiers and the error rate are descendant when it is being related to the prevailing technique.

DOI: 10.37200/IJPR/V24I5/PR201795
Received: 13 Feb 2020 | Revised: 07 Mar 2020 | Accepted: 23 Mar 2020

International Journal of Psychosocial Rehabilitation, Vol. 24, Issue 05, 2020
ISSN: 1475-7192

Brain Tumor Cross Validation

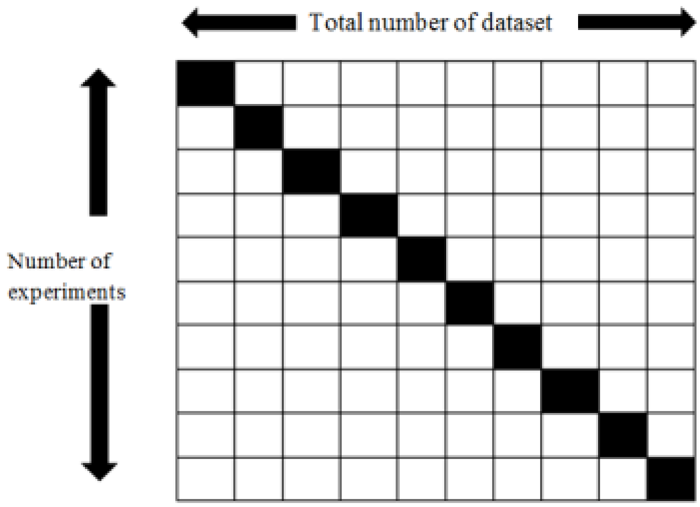

Fig. 11: Basic k-folds for Database Cross Validation

The present challenging situation is to take a decision about the number of folds required. If K value is taken too large, then bias will be small of the "true error rate estimator", but large will be the variance of the estimator and its time-consumption is more. Alternatively, if small the K, there will be a decrease in time computation, variance of the estimator is small, but more will be the estimator bias [40].

By observing the plot in figure 12, which is the effect of the cross validation on different algorithm compared with semantic segmentation based nano technique. We can say that the 6 cross validation (ostu's, morphological operation, region growing, K-means clustering and the proposed semantic segmentation based Nano technique) of all the segmentation kernel behavior is horizontal and the proposed algorithm is utilized as it gives high classification accuracy for the given data set as shown in the Fig.12.

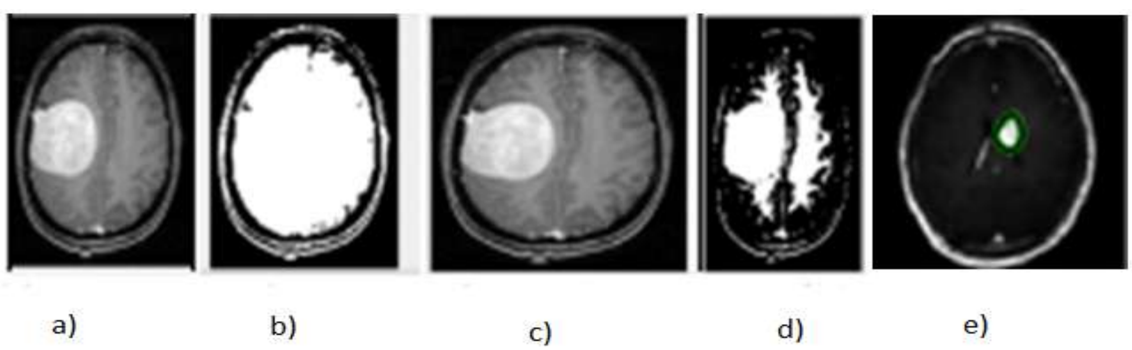

Fig. 12: The MRI Images a) Ostu's Segmentation b) Morphological Operation c) Region Growing d) K-means Clustering and e) Proposed Semantic Segmentation based Nano Technique with 6-cross Validation

A system that detects Tumour by deep learning technique. This system provides are al-time solution to the diagnostics of tumour in brain tumor cell. This proposed system has an average accuracy rate. The result of the proposed model is that we can use ResNet architecture to differentiate the affected tumour cells.

DOI: 10.37200/IJPR/V24I5/PR201795
Received: 13 Feb 2020 | Revised: 07 Mar 2020 | Accepted: 23 Mar 2020

International Journal of Psychosocial Rehabilitation, Vol. 24, Issue 05, 2020
ISSN: 1475-7192

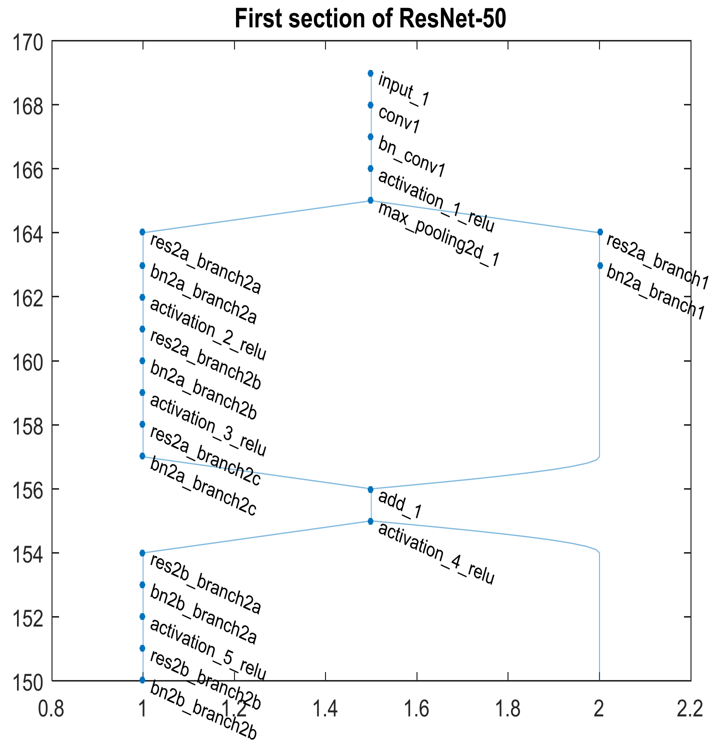

Fig. 13: Resnet 50 Architecture

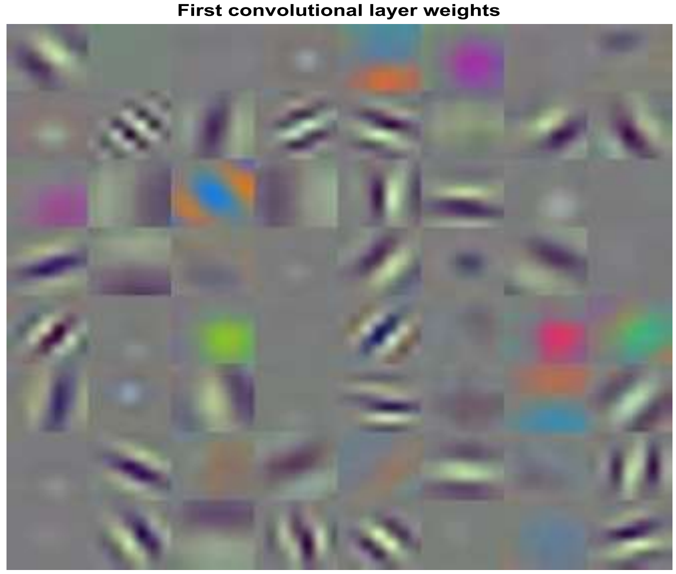

Fig. 14: Output of CNN Classifiers

Confusion matrix is the graphical representation between the Target class and Output class. In this matrix the true positive values are denoted as green color box and the true negative valve are shows in red box. Fig. 14 shows the output of CNN classifiers which are the customary metrics morals for numerous features. It is possible to recognize from table, which feature amalgamations provides higher accuracy. Border error symbolizes the rate of faultily brain images. This gives the lower accuracy of 90.00%.

DOI: 10.37200/IJPR/V24I5/PR201795
Received: 13 Feb 2020 | Revised: 07 Mar 2020 | Accepted: 23 Mar 2020

Table 5: Analysis of Performances Parameters

Method	Accuracy (%)	Sensitivity (%)	Specificity (%)	PSNR	MSE
Region Growing	84.92	75.23	84.88	54.75	2.2114
Watershed	77.11	82.16	76.98	42.25	3.4968
proposed semantic segmentation based Nano technique	94.13	90.59	91.12	68.19	2.3998

As per the obtained outputs, it is clear that Canny edge detector segments tumor regions more similar to the existing images. Accuracy is an important parameters of a segmentation algorithm. Watershed algorithm has the lowest segmentation accuracy of 77.11% and highest segmentation accuracy of 94.13% is obtained for canny edge detector. The accuracy of the region growing is 84.92%. Thus, from this comparison it is well cleared that proposed algorithm is the superior algorithm in terms of classification accuracy.

V. Conclusion

The keystone of this scrutiny recognizes the brain nodules using semantic segmentation based Nano algorithm which in turn augments the quality of images. Isolateral filter is used for brain MRI scan images for noise elimination and the numerous validity actions relate to the preferred noise removal methods. The preprocessed brain MRI images undergo the computation of three miscellaneous performance measures (comprising of PSNR, MSE, and SSIM). The solitary nodules are procured using Advanced CNN. The efficiency of the data set is evaluated by virtue of classification accuracy. The highest classification accuracy is recorded in the confusion matrices. The proposed Advanced CNN have auspiciously engendered 95.7% of accuracy. The propounded methodology exhibits ameliorated sensitivity and diminished computation time. An early diagnosis can substantially ameliorate the survival chance of patients. Consequently, the proposed methodology manifest that the advanced CAD system has outstanding potential for automatic diagnosis of brain tumor. This work and the results do not refrain the line of research. The main constraint of the proposed methodology for brain lesion segmentation omits the segmentation area calculated accurately due to the variation of shape and size of this nodule. The future scope of the work emphasizes the innovative method to detect the accurate location of these types of brain nodules is continuing to demand.

References

[1] Zhuang, Audrey H., Daniel J. Valentino, and Arthur W. Toga. "Skull-stripping magnetic resonance brain images using a model-based level set." *NeuroImage* 32, no. 1 (2006): 79-92.

[2] Carass, Aaron, Jennifer Cuzzocreo, M. Bryan Wheeler, Pierre-Louis Bazin, Susan M. Resnick, and Jerry L. Prince. "Simple paradigm for extra-cerebral tissue removal: algorithm and analysis." *NeuroImage* 56, no. 4 (2011): 1982-1992.

[3] Chaddad, Ahmad, and Camel Tanougast. "Quantitative evaluation of robust skull stripping and tumor detection applied to axial MR images." *Brain informatics* 3, no. 1 (2016): 53-61.

[4] Mohsin, Sajjad, Sadaf Sajjad, Zeeshan Malik, and Abdul Hanan Abdullah. "Efficient way of skull stripping in MRI to detect brain tumor by applying morphological operations, after detection of false background." *International Journal of Information and Education Technology* 2, no. 4 (2012): 335.

[5] Somasundaram, K., and P. Kalavathi. "Skull stripping of MRI head scans based on chan-vese active contour model." *KM&EL* 3 (2011): 7-14.

[6] Ségonne, Florent, Anders M. Dale, Evelina Busa, Maureen Glessner, David Salat, Horst K. Hahn, and Bruce Fischl. "A hybrid approach to the skull stripping problem in MRI." *Neuroimage* 22, no. 3 (2004): 1060-1075.

DOI: 10.37200/IJPR/V24I5/PR201795
Received: 13 Feb 2020 | Revised: 07 Mar 2020 | Accepted: 23 Mar 2020

[7] Rex, David E., David W. Shattuck, Roger P. Woods, Katherine L. Narr, Eileen Luders, Kelly Rehm, Sarah E. Stolzner, David A. Rottenberg, and Arthur W. Toga. "A meta-algorithm for brain extraction in MRI." *NeuroImage* 23, no. 2 (2004): 625-637.

[8] Balan, Andre GR, Agma JM Traina, Marcela X. Ribeiro, Paulo MA Marques, and Caetano Traina Jr. "Smart histogram analysis applied to the skull-stripping problem in T1-weighted MRI." *Computers in Biology and Medicine* 42, no. 5 (2012): 509-522.

[9] Wood, Michael L., and V.M. Runge. "Application of image enhancement techniques to magnetic resonance imaging." *Radiographics* 8, no. 4 (1988): 771-784.

[10] Haney, Sean M., Paul M. Thompson, Timothy F. Cloughesy, Jeffry R. Alger, and Arthur W. Toga. "Tracking tumor growth rates in patients with malignant gliomas: A test of two algorithms." *American Journal of Neuroradiology* 22, no. 1 (2001): 73-82.

[11] Tzika, A. Aria, Maria K. Zarifi, Liliana Goumnerova, Loukas G. Astrakas, David Zurakowski, Tina Young-Poussaint, Douglas C. Anthony, R. Michael Scott, and Peter McL Black. "Neuroimaging in pediatric brain tumors: Gd-DTPA–enhanced, hemodynamic, and diffusion MR imaging compared with MR spectroscopic imaging." *American journal of neuroradiology*23, no. 2 (2002): 322-333.

[12] Chen, Zhe, David Dagan Feng, and WeidongCai. "Automatic detection of PET lesions." In *Selected papers from the 2002 Pan-Sydney workshop on Visualisation-Volume 22*, pp. 21-26. Australian Computer Society, Inc., 2003.

[13] Boada, Fernando E., Denise Davis, Kevin Walter, Alejandro Torres-Trejo, Douglas Kondziolka, Walter Bartynski, and Frank Lieberman. "Triple quantum filtered sodium MRI of primary brain tumors." In *Biomedical Imaging: Nano to Macro, 2004. IEEE International Symposium on*, pp. 1215-1218. IEEE, 2004.

[14] Prastawa, Marcel, Elizabeth Bullitt, and Guido Gerig. "Simulation of brain tumors in MR images for evaluation of segmentation efficacy." *Medical image analysis* 13, no. 2 (2009): 297-311.

[15] Sebe, Nicu, and Michael S. Lew. "Wavelet based texture classification." In *Pattern Recognition, 2000. Proceedings. 15th International Conference on*, vol. 3, pp. 947-950. IEEE, 2000.

[16] Jiang, Chunyan, Xinhua Zhang, Wanjun Huang, and Christoph Meinel. "Segmentation and quantification of brain tumor." In *Virtual Environments, Human-Computer Interfaces and Measurement Systems, 2004.(VECIMS). 2004 IEEE Symposium on*, pp. 61-66. IEEE, 2004.

[17] Yang, Yong, and Shuying Huang. "Novel statistical approach for segmentation of brain magnetic resonance imaging using an improved expectation maximization algorithm." *OpticaApplicata* 36, no. 1 (2006): 125.

[18] Morris, Marianne, Russell Greiner, Jörg Sander, Albert Murtha, and Mark W. Schmidt. "Learning a Classification-based Glioma Growth Model Using MRI Data." *JCP* 1, no. 7 (2006): 21-31.

[19] Zhang, Bo, Jalal M. Fadili, and Jean-Luc Starck. "Wavelets, ridgelets, and curvelets for Poisson noise removal." *IEEE Transactions on Image Processing* 17, no. 7 (2008): 1093-1108.

[20] Ratan, Rajeev, Sanjay Sharma, and S. K. Sharma. "Brain tumor detection based on multi-parameter MRI image analysis." *ICGST-GVIP Journal* 9, no. 3 (2009): 9-17.

[21] Abdel-Maksoud, Eman, Mohammed Elmogy, and Rashid Al-Awadi. "Brain tumor segmentation based on a hybrid clustering technique." *Egyptian Informatics Journal* 16, no. 1 (2015): 71-81.

[22] Mayer, Arnaldo, and Hayit Greenspan. "An adaptive mean-shift framework for MRI brain segmentation." *IEEE Transactions on Medical Imaging* 28, no. 8 (2009): 1238-1250.

[23] Li, Yuhong, FucangJia, and Jing Qin. "Brain tumor segmentation from multimodal magnetic resonance images via sparse representation." *Artificial intelligence in medicine* 73 (2016): 1-13.

[24] Tustison, Nicholas J., Brian B. Avants, Philip A. Cook, Yuanjie Zheng, Alexander Egan, Paul A. Yushkevich, and James C. Gee. "N4ITK: improved N3 bias correction." *IEEE transactions on medical imaging* 29, no. 6 (2010): 1310-1320.

[25] Nyúl, László G., Jayaram K. Udupa, and Xuan Zhang. "New variants of a method of MRI scale standardization." *IEEE transactions on medical imaging* 19, no. 2 (2000): 143-150.

[26] Gupta, Nidhi, and Rajib K. Jha. "Enhancement of dark images using dynamic stochastic resonance with anisotropic diffusion." *Journal of Electronic Imaging* 25, no. 2 (2016): 023017.

[27] Pham, Dzung L., Chenyang Xu, and Jerry L. Prince. "Current methods in medical image segmentation." *Annual review of biomedical engineering* 2, no. 1 (2000): 315-337.

[28] Lee, Chulhee, Shin Huh, Terence A. Ketter, and Michael Unser. "Unsupervised connectivity-based thresholding segmentation of midsagittal brain MR images." *Computers in biology and medicine* 28, no. 3 (1998): 309-338.

[29] Held, Karsten, E. Rota Kops, Bernd J. Krause, William M. Wells, Ron Kikinis, and H-W. Muller-Gartner. "Markov random field segmentation of brain MR images." *IEEE transactions on medical imaging* 16, no. 6 (1997): 878-886.

[30] Zhang, Yongyue, Michael Brady, and Stephen Smith. "Segmentation of brain MR images through a hidden Markov random field model and the expectation-maximization algorithm." *IEEE transactions on medical imaging* 20, no. 1 (2001)

[31] Suda, I.K. (2017). The children character improvement through painting activities in art school: I Wayan Gama Painting School. *International Research Journal of Management, IT and Social Sciences,* 4(4), 11-21.

[32] Sriartha, I.P., & Giyarsih, S.R. (2017). Subak endurance in facing external development in South Bali, Indonesia. *International Research Journal of Management, IT and Social Sciences*, 4(4), 22-34.

[33] Kusum, P.A., & Yinghua, S. (2017). Effectiveness of on-the-job learning for enterprises' innovativeness. *International Research Journal of Management, IT and Social Sciences,* 4(4), 35-43.

[34] Ljupco, N., & Jasminka, N. (2017). Unemployment an unauthorized unique road about apathy and poverty the Macedonian man without knowledge and skills. *International Research Journal of Management, IT and Social Sciences,* 4(4), 44-57.

[35] Suweken, G., Waluyo, D., & Okassandiari, N.L. (2017). The improvement of students' conceptual understanding and students' academic language of mathematics through the implementation of SIOP model. *International Research Journal of Management, IT and Social Sciences,* 4(4), 58-69.

[36] Suganya, M., & Anandakumar, H. (2013). Handover based spectrum allocation in cognitive radio networks. 2013 International Conference on Green Computing, Communication and Conservation of Energy (ICGCE). doi:10.1109/icgce.2013.6823431

[37] Anandakumar, H., & Umamaheswari, K. (2017). An Efficient Optimized Handover in Cognitive Radio Networks using Cooperative Spectrum Sensing. *Intelligent Automation & Soft Computing,* 1–8.

[38] Haldorai, A., Ramu, A., & Murugan, S. (2018). Social Aware Cognitive Radio Networks. *Social Network Analytics for Contemporary Business Organizations,* 188–202.

[39] Haldorai, A., & Kandaswamy, U. (2019). Supervised Machine Learning Techniques in Intelligent Network Handovers. *EAI/Springer Innovations in Communication and Computing,* 135–154.

[40] Haldorai, A., Ramu, A., & Murugan, S. (2018). Social Aware Cognitive Radio Networks. *Social Network Analytics for Contemporary Business Organizations,* 188–202.

[41] Sharma, A. (2015). Key Highlights of the Companies Act, 2013- Incorporation of the Companies. *International Journal of Advanced Engineering, Management and Science,* 1(5), pp.01-04.

[42] Mandal, D. and Hussain, A. (2015). An Insight into the Governance of Indian Universities since 20th Century. *International Journal of Advanced Engineering, Management and Science,* 1(5), pp.05-09.

[43] Babu, A., Haile, A. and Viswanath, C. (2015). Application of Load Following Control in Multi Area Hydrothermal Gas System under Reconstituted Scenario. *International Journal of Advanced Engineering, Management and Science,* 1(5), pp.10-15.

[44] Singh, J., Bhuddhi, D., Singh, M., & Rajpoot, M. (2016). Experimental Study on Effect of PCM Material used in Chocolate Freezer. *International Journal of Advanced Engineering Research and Science,* 3(9), 205-210.

[45] Rani, N. (2016). Implementation of DWT Integrated Log Based FPU with SPIHT Coders on FPGA. *International Journal of Advanced Engineering Research and Science,* 3(9), 211-216.

[46] Gupte, A., Naganarayanan, A., & Krishnan, M. (2016). Emotion Based Music Player - XBeats. *International Journal of Advanced Engineering Research and Science,* 3(9), 217-223.

[47] Wamoto, J., Ayuma, D., & Chege, P. (2016). Entrepreneurial Factors Influencing the Performance of Government Funded Youth Group Enterprises in Turbo Sub-County Uasin Gishu County - Kenya. *International Journal of Advanced Engineering Research and Science,* 3(9), 224-235.

[48] Suman Rajest S, Dr. P. Suresh, "The white Tiger by Aravind Adiga: Depiction of Fermentation in Society" in *International Journal of Information Movement (IJIM),* Volume: II, Special Issue VI, October 2017, Page No.: 189-194.

[49] Suman Rajest S, Dr. P. Suresh, "Confrontation on Modernism or Postmodernism Changes after the World War" in New Academia: An *International Journal of English Language, Literature and Literary Theory,* Volume: VII, Special Issue I, January 2018, Page No.: 50-76.

[50] Dr. P.S. Venkateswaran, Dr. A. Sabarirajan, S. Suman Rajest and R. Regin (2019) "The Theory of the Postmodernism in Consumerism, Mass Culture and Globalization" in *The Journal of Research on the Lepidoptera* Volume 50 (4): 97-113

DOI: 10.37200/IJPR/V24I5/PR201795
Received: 13 Feb 2020 | Revised: 07 Mar 2020 | Accepted: 23 Mar 2020

[51] Desfiandi, A., Suman Rajest, S., S. Venkateswaran, P., Palani Kumar, M., & Singh, S. (2019). Company Credibility: A Tool to Trigger Positive CSR Image in the Cause-Brand Alliance Context in Indonesia. *Humanities & Social Sciences Reviews*, 7(6), 320-331.

[52] Rajest, S.S., Suresh, D. (2018). The Deducible Teachings of Historiographic Metafiction of Modern Theories of Both Fiction and History. *Eurasian Journal of Analytical Chemistry,* 13(4), emEJAC191005.

[53] K.B. Adanov, S. Suman Rajest, Mustagaliyeva Gulnara, Khairzhanova Akhmaral (2019). "A Short View on the Backdrop of American's Literature". *Journal of Advanced Research in Dynamical and Control Systems,* Vol. 11, No. 12, pp. 182-192.

[54] Dr.P. Suresh and Suman Rajest S (2019). "An Analysis of Psychological Aspects in Student-Centered Learning Activities and Different Methods" in *Journal of International Pharmaceutical Research,* Volume: 46, Issue 01, Page No.: 165-172.

[55] Md. Salamun Rashidin, Sara Javed, Bin Liu, Wang Jian, Suman Rajest S. "Insights: Rivals Collaboration on Belt and Road Initiatives and Indian Recourses" in *Journal of Advanced Research in Dynamical and Control Systems,* Volume: 11, Special Issue 04, 2019, Page No.: 1509-1522.

DOI: 10.37200/IJPR/V24I5/PR201795
Received: 13 Feb 2020 | Revised: 07 Mar 2020 | Accepted: 23 Mar 2020